Desalination and Water Treatment
www.deswater.com

doi: 10.1080/19443994.2013.797673

52 (2014) 3206–3218
April

Taylor & Francis
Taylor & Francis Group

High capacity removal of silver(I) and lead(II) ions by modified polyacrylonitrile from aqueous solutions

Gholamreza Kiani[a,*], Mehdi Soltanzadeh[b]

[a]*School of Engineering-Emerging Technologies, University of Tabriz, Tabriz, Iran*
Tel. +98 4113393853; Fax: +98 4113294626; email: g.kiani@tabrizu.ac.ir
[b]*Department of Engineering, Ahar branch, Islamic Azad University, Ahar, Iran*

Received 1 August 2012; Accepted 10 April 2013

ABSTRACT

Different polymeric materials carrying synthetic adsorbents have been reported in literature for heavy metal removal. We have developed a simple method for functionalizing of polyacrylonitrile (PAN) with two volume percent (50 and 100) of triethylenetetramine (PAN–TETA 50 and 100). For the first time, PAN–TETA was used as an absorbent of silver and lead ions from aqueous solutions. PAN–TETA and their metal complexes have been studied by FT-IR and scanning electron microscope. The analysis method confirmed the presence of metal in PAN–TETA complexes. The prepared functionalized PAN were applied to remove heavy metal ions, such as Pb(II) and Ag(I) from aqueous solutions. The optimization of experimental conditions and parameters including initial pH, contact time, adsorbent dose, initial metal and ions concentration, and temperature for the removal of heavy metals were investigated. The adsorption increased with increasing metal ions concentration, initial pH, and temperature. Pseudo-first-order, pseudo-second-order, and intraparticle diffusion models were considered to evaluate the rate parameters. The adsorption followed pseudo-second-order kinetic model with correlation coefficients greater than 0.997. Attempts were made to fit the isothermal data using Langmuir, Freundlich, and Temkin equations. The maximum sorption capacity of $108.14\,\mathrm{mg\,g^{-1}}$ and $99.01\,\mathrm{mg\,g^{-1}}$ for silver and lead ions were achieved at $\mathrm{pH}=6$, respectively. The values of thermodynamic parameters of ΔG°, $\Delta H,^\circ$ and ΔS° indicated that the adsorption process was spontaneous and endothermic. The selectivity of two PAN–TETA for the adsorption of Ag(I) and Pb(II) were studied. The competitive adsorption tests verified that these functionalized polymers have good adsorption selectivity for Ag(I) with the coexistence of two ions. Desorption of the metal ions from PAN–TETA was studied in 0.5 M HCl and very high desorption rates, greater than 91%, were achieved in all cases. Based on adsorption/desorption data, PAN–TETA is a promising adsorbent for heavy metals removal from the aqueous medium.

Keywords: Polyacrylonitrile; Triethylenetetramine; Adsorption; Kinetic model; Thermodynamic parameter; Heavy metal ions

1. Introduction

Functionalization of various adsorbents for the removal of heavy metal ions from water or wastewater has attracted great research interest in recent years due to the advantages of achieving high efficiency and good selectivity. Environmental pollution caused by toxic heavy metals is one of the most hazardous problems in many densely populated cities worldwide.

---

*Corresponding author.

The industrial and domestic wastes responsible for various damages to the environment adversely affect the health of the human population. Several events resulting from heavy metal contamination in the aquatic environment have increased the awareness of the heavy metal toxicity [1].

It is well known that polymeric materials with complex ligands containing sulfur, nitrogen, and oxygen atoms have excellent sorption selectivity for transition metal cations due to the strong affinity between sulfur, nitrogen, oxygen atoms, and metal ions. Several functional groups, such as diethylene-triaminetetraacetic [2], monoethanolamine [3], diethylenetriamine [4], and ethylenediaminetetraacetic acid [5] have been used for metal ions adsorption. These introduced functional groups will modify the chemical composition of the polymeric matrix surface, hence improve their adsorption behavior. Among these chelating ligands, linear polyamine can often form stable metal complexes with a variety of metal ions and triethylenetetramine (TETA) is one of them [6].

Various methods exist for the removal of heavy metal ions from wastewater, which include chemical precipitation/coagulation, membrane technology, electrolytic reduction, ion exchange, and adsorption [7]. Adsorption is commonly used to remove heavy metal ions from aqueous solutions at trace concentrations. Attachment of metal ions to the sorbent surfaces may be due to various physical or chemical interactions (ion exchange or chelating mechanism) between the metal ions and the surface functional groups of sorbent.

To improve the metal-adsorption capacity of polymeric materials, it may be modified as reported by some workers. TETA has been used for the modification of some materials, such as: poly(glycidyl methacrylate-co-trimethylolpropane trimethacrylate) [8], polystyrene resin [9], succinylated-mercerized-cellulose [10], and poly(glycidyl methacrylate) (PGMA) [11]. It has been found that the functionalized materials can easily adsorb heavy ions from aqueous solutions.

To the best of our knowledge, there are a few studies relevant to silver ions adsorption. Modified PAN adsorbents, such as activated PAN–DTA [4], chitosan/cellulose [12], and hitosan/magnetite [13] for heavy metal ions have been investigated. In this study, PAN was further used as the substrate for functionalization. Aliphatic polyamine of TETA increased molecular lengths and thus a number of amine groups were used to functionalize PAN as adsorbents and the adsorbents were examined for their properties and performance in silver and lead ions removal. The focus included the increase of amine content of adsorbents in silver and lead ions adsorption. The effects of adsorbent dose, initial pH, temperature, initial metal ions concentration, and contact time were investigated. The equilibrium, kinetic data, and thermodynamic parameters were processed to understand the adsorption mechanism of heavy metal ions onto PAN–TETA.

2. Experimental details

2.1. Materials

Polyacrylonitrile (PAN) powder was provided by Polyacryl Co. (Isfahan, Iran) with a molecular weight of 60,000 g mol^{-1} (15% methylacrylate (MA), based on elemental analysis data). TETA was purchased from Merck and used without purification. Nitrate salts of metal ions were provided by Fluka and used as received. The FT-IR spectra (500–4,000 cm^{-1}) and electron micrographs were obtained from Unicom 4,600 spectrophotometer using KBr pellets and scanning electron microscope (SEM) ZEISS DSM 960, respectively. The metal adsorption capacities of polymers were measured by atomic adsorption spectrophotometer (AA 55B, Varian SLM) at room temperature.

2.2. Adsorption experiments

The 100 mL samples containing known concentration of metal ion and PAN–TEAT were added to Erlenmeyer flasks. The flasks were stirred with a rate of 300 rpm in a water bath (Pars Azma, Iran). The pH of the metal ions solutions was adjusted in the range of 4–6 with 0.1 N HCl or 0.1 N NaOH within a WTW pH 3,110 SET 2 pH-meter with a combined pH electrode. Competitive heavy metal adsorption from aqueous solutions containing Ag(I) and Pb(II) were investigated by the aforementioned procedure.

The amounts of metal ions adsorbed on PAN–TETA for every time, t were calculated from the concentrations in solutions before and after adsorption. The amount of metal ions adsorbed (mg g^{-1}) (q_t) by PAN–TETA for every t were calculated from the mass balance equation as follows:

$$q_t = V(C_0 - C_t)/W \tag{1}$$

where q_t is the amount of metal ions adsorbed into PAN–TETA at any time (mg g^{-1}), C_0 and C_t are the concentrations of metal ions before adsorption and after contact time (mg L^{-1}), respectively; V is the volume of metal ions solution (L), and W is the mass of PAN–TETA sample (g) [14,15].

In order to determine the best kinetic model that fits the adsorption experimental data, the pseudo-first-order, pseudo-second-order, and intraparticle diffusion models were examined. The linear forms of these models can be described as follows.

$$\ln(q_e - q_t) = \ln q_e - k_1 t \tag{2}$$

$$\frac{t}{q_t} = \frac{1}{k_2 q_e^2} + \frac{1}{q_e} t \tag{3}$$

$$q_t = k_i t^{1/2} \tag{4}$$

where q_e is the amount of the adsorbed pollutant at equilibrium per unit mass of the adsorbent (mg g^{-1}); k_1 (min^{-1}), k_2 (g $\text{mg}^{-1}\,\text{min}^{-1}$), and k_i (mg $g^{-1}\,\text{min}^{-1/2}$) are the rate constants of the adsorption in pseudo-first-order (Eq. (2)), pseudo-second-order (Eq. (3)), and intraparticle diffusion models (Eq. (4)), respectively [16–18]. Each experiment was run in triplicate and the mean values were reported. Standard deviations were found to be within ±1.3%. Further, the error bars for the figures were so small that they were smaller than the symbols used to plot the graphs and hence, not shown.

2.3. Ion exchange capacity and swelling behavior of PAN–TETA

Ion exchange capacity of PAN–TETA was performed according to literature [19]. Swelling measurement of PAN–TETA was done as follows: PAN–TETA (0.10 g) was put into a weighed tea bag, immersed in 100 mL distilled water, and allowed to soak for 2 h at room temperature. The equilibrated swollen gel was allowed to drain by removing the tea bag from water and hanging until no more drop drained (20 min). The bag was then weighed to determine the weight of the swollen PAN–TETA. The absorbency (equilibrium swelling) was calculated using the following equation:

$$\text{Absorbency} = (W_s - W_d)/W_d \tag{5}$$

where W_s and W_d are the weights of the swollen PAN–TETA and the dry sample, respectively [20]. So, the absorbency was calculated as grams of water per gram of PAN–TETA (g g^{-1}).

2.4. Desorption studies

Desorption studies help to elucidate the nature of adsorption, recycling of the spent adsorbent, and the metal ions. The effect of various reagents used for desorption are studied. Three cycles of adsorption and desorption were performed to study the reusability of the sorbent. Desorption of metal ions was performed with 0.1 M HCl solution.

2.5. Preparation of PAN–TETA 50

PAN–TETA 50 was prepared by adding a 2.5 g amount of PAN to 25 mL of 50% (v/v in water) TETA solution in a 100 mL round bottom flask. The mixture was stirred on a magnetic stirrer and the reaction was allowed to proceed at 100–110°C for 24 h. Then, the PAN–TETA was separated from the solution through filtration and then rinsed with distilled water till neutralization. The product was dried at 50°C in an oven overnight and stored in a desiccators prior to use for the sorption study. PAN–TETA100 was prepared similar to the above procedure using 100% TETA (v/v in water) aqueous solutions [19].

Two different types of PAN–TETA have been investigated for two heavy metal ions. Various numbers of graphs have been extracted and rest of the data has been inserted in Tables.

3. Results and discussion

3.1. Analysis of FT-IR spectra

Fig. 1 shows the FT-IR spectra of the raw PAN and prepared PAN–TETA. The FT-IR spectrum of the raw PAN (Fig. 3(a)) shows the peaks at 3,528 cm^{-1} (OH stretching), 2,242 cm^{-1} (C≡N stretching), 2,938 cm^{-1} (CH stretching in CH, CH_2 and CH_3 groups), 1,072 cm^{-1} (C–H bending), and 1,732 cm^{-1} (C=O stretching) confirming the original powder as a copolymer of acrylonitrile and MA. After the reaction of PAN with two volume percent of TETA, the spectra of the obtained functionalized-PAN in (Fig. 3(b) and (c)) show many significant changes. With an increase in volume percent of TETA (50%), the peak at 2,245 cm^{-1} for the C≡N stretching did not disappear completely, which suggests that only some part of the nitrile groups on the PAN were converted during the treatment (Fig. 1(b)). On the other hand, in 100% of TETA, the peak at 2,245 cm^{-1} disappears completely (Fig. 1(c)). In addition, the new bonds observed at 1,651, 1,556, 1,597, and 1,381 cm^{-1} for the PAN–TETA can be assigned to the C=O (or C=N) groups in amide, the N–H group in amine or amide, and the C–N group in amide, respectively. These results confirm that PAN structure functionalized with TETA (Fig. 8).

Table 1 shows details of the FT-IR adsorption signals for PAN–TETA (50 and 100) with respect to their Ag(I) and Pb(II) complexes. By comparing data in Table 1, it can be seen that many significant changes appeared. For instance, after metal ions sorption, the peaks of N–H stretching at 3,394 and 3,371 cm^{-1} for PAN–TETA 50 and PAN–TETA 100, respectively, shifted towards higher wave number.

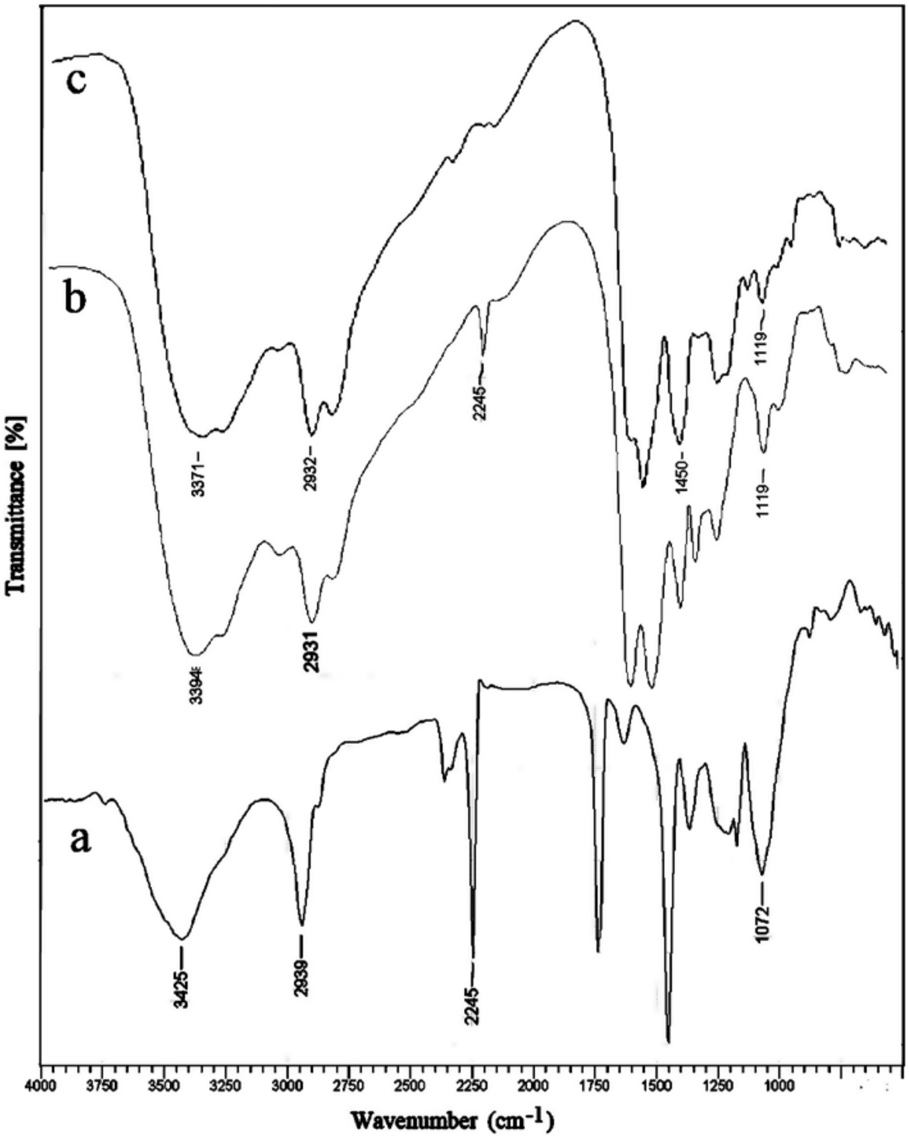

Fig. 1. FT-IR spectra of (a) PAN, (b) PAN–TETA 50, and (c) PAN–TETA 100.

Also, the peak at 1,057 cm^{-1} of C–H bending was shifted towards higher wave numbers. These changes confirm Ag(I) and Pb(II) ions to form chelate complexes with PAN–TETA [19].

3.2. *Effect of experimental conditions on removal of silver and lead ions*

3.2.1. *Effect of pH*

The pH of the aqueous solution is one of the important controlling parameters that affect the adsorption process [21]. The selected pH values in the experiments were prior to the precipitation limit of the metal ions. As shown in Fig. 2, the higher uptake capacity was achieved at higher pH values. The observed lower uptake in an acidic medium may be attributed to the partial protonation of the active groups and the competition of H^+ with metal ions for adsorption sites on the PAN–TETA. The results indicate that the adsorption percent of Ag(I) is higher than that of Pb(II) ion in applied pH ranges suggesting possible selectivity for this metal ion.

3.2.2. *Effect of contact time and initial metal ions concentration*

The effect of initial metal ions concentration and contact time on the adsorption rate of metal ions onto PAN–TETA is shown in Fig. 3. The amount of silver ion adsorbed at any time increases from 0.452 to 1.01 $\mathrm{m\,mol\,g}^{-1}$ (48.38–108.14 $\mathrm{mg\,g}^{-1}$) by increasing the

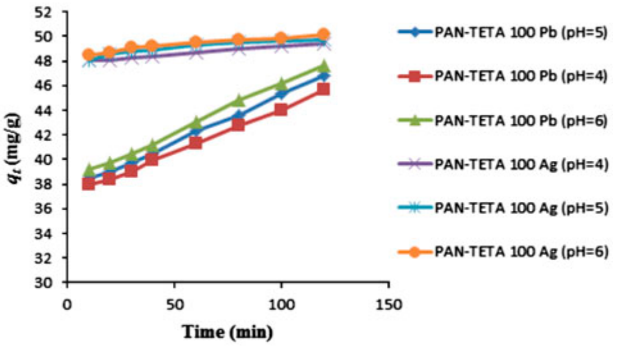

Fig. 2. Effect of contact time and initial pH on the removal rate of silver and lead ions onto PAN–TETA from aqueous solutions ($T = 20$°C, [metal ion]$_0 = 50\,\mathrm{mg\,L^{-1}}$, PAN–TETA = 0.1 g).

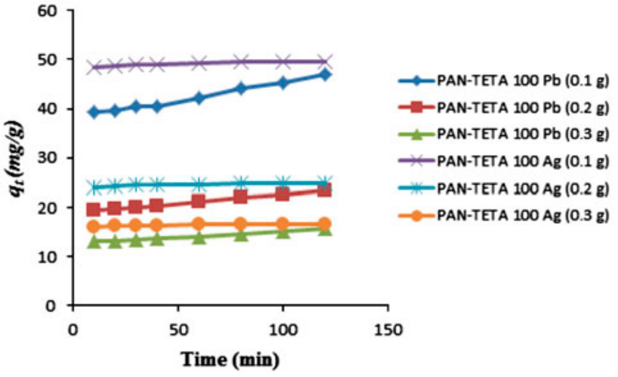

Fig. 3. Effect of adsorbent dose on adsorption of silver and lead ions onto PAN–TETA ($T = 20$°C, [metal ions]$_0 = 50\,\mathrm{mg\,L^{-1}}$, pH = 6).

initial silver ion concentration from 50 to 110 mg $\mathrm{L^{-1}}$. Therefore, adsorption increases with the increasing initial metal ion concentration. The results show that uptake of metal ions is rapid for the first 20 min, reaching equilibriumin about 30 min.

3.2.3. Effect of adsorbent dose

Adsorbent dose is a significant parameter in the determination of adsorption capacity. In order to study the effect of adsorbent mass on the adsorption of metal ions, a series of adsorption experiments was carried out via different adsorbent dosages at initial metal ions concentration of 50 mg $\mathrm{L^{-1}}$. Fig. 4 shows the effect of adsorbent dose on the removal of silver and lead ions. This reveals that the instantaneous and equilibrium sorption capacities of metal ions are functions of the PAN–TETA dosage. Along with the increase of adsorbent dose from 0.1 to 0.3 g, sorption capacity of metal ions decreased from 48.18 to 16.03 mg $\mathrm{g^{-1}}$. This may be attributed to the aggregation of adsorbent particles at high dosage, which reduces the total surface area of the adsorbent and results in an increase in the diffusion path length. Also, increasing the dosage of PAN–TETA and keeping the metal ions concentration constant makes a large number of sites available for a fixed concentration of sorbate, hence the reduction in the value of q_t [22].

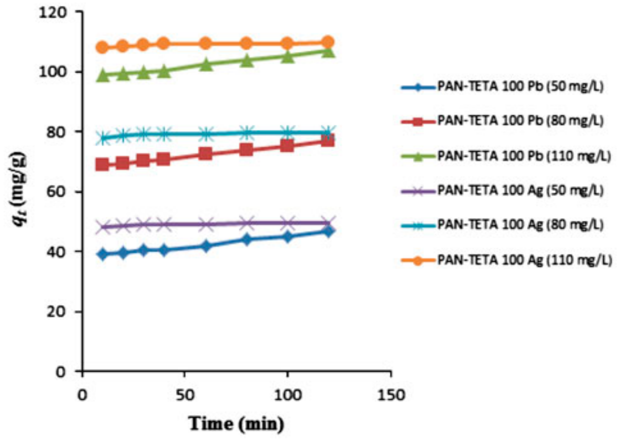

Fig. 4. Effect of contact time and initial concentration of silver and lead ions onto PAN–TETA from aqueous solutions ([metal ions]$_0 = 50$, 80 and 110 mg $\mathrm{L^{-1}}$, $T = 20$°C, pH = 6).

3.2.4. Effect of temperature

To study the effect of temperature on the adsorption of metal ions adsorption by PAN–TETA, the experiments were performed at temperatures of 293, 308, and 323 K. Fig. 5 shows the influence of temperature on the adsorption of Ag(I) and Pb(II) onto modified PAN. As it was observed, the equilibrium adsorption capacity of metal ions onto PAN–TETA was found to increase with temperature increment, especially in higher equilibrium concentrations, or

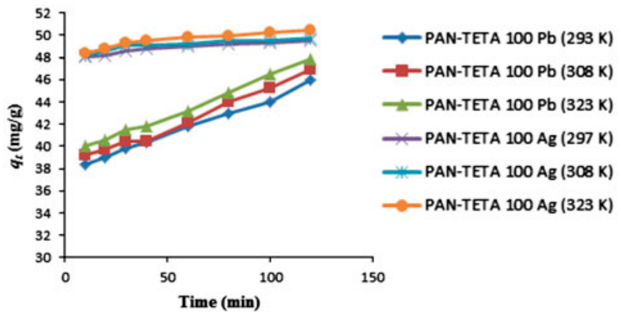

Fig. 5. Effect of contact time and temperature on the removal efficiency of silver and lead ions onto PAN–TETA from aqueous solutions ([metal ions]$_0 = 50\,\mathrm{mg\,L^{-1}}$, pH = 6, PAN–TETA = 0.1 g).

lower adsorbent doses because of high driving force of adsorption. This fact indicates that the mobility of metal ion-fetched molecules increased with the temperature increment. The adsorbent shows the endothermic nature of adsorption.

3.2.5. *Effect of ionic strength*

The ionic strength of the solution is of significance for its effect on the adsorbent, as well as the adsorbate. To determine the effect of ionic strength on Pb(II) adsorption, equilibrium adsorption studies were carried out. The experiments were done in the presence of varying chloride environments using various chloride solutions. While experimenting, the absence of other anions has ensured that the adsorbed amount at equilibrium increased with an increase in ionic strength. The effect of sodium chloride on the adsorption of lead ion onto PAN–PETA 100 is shown in Fig. 6. According to the surface chemistry theory developed by Guoy–Chapman, when a PAN–TETA is in contact with sorbate species in solution, they will be surrounded by an electrical diffused double layer. The thickness of the latter will be significantly compressed by the presence of NaCl [23]. Such compression helps the PAN–TETA molecules and Cd(II) species to approach each other more closely and the increased electrostatic attraction results in the increased uptake of Cd(II) ion.

3.3. *Preparation of PAN–TETA*

The interaction of TETA with PAN and experimental conditions are illustrated in Fig. 7. The prepared functionalized-PAN was insoluble in water and common organic solvents, suggesting the formation of a cross-linking structure. Also, SEM was used to study PAN–TETA and its metal complex morphology. It is obvious that in the presence of TETA, the porosity of PAN–TETA Ag and PAN–TETA Pb in comparison with PAN is increased (Fig. 8(a) and (b)).

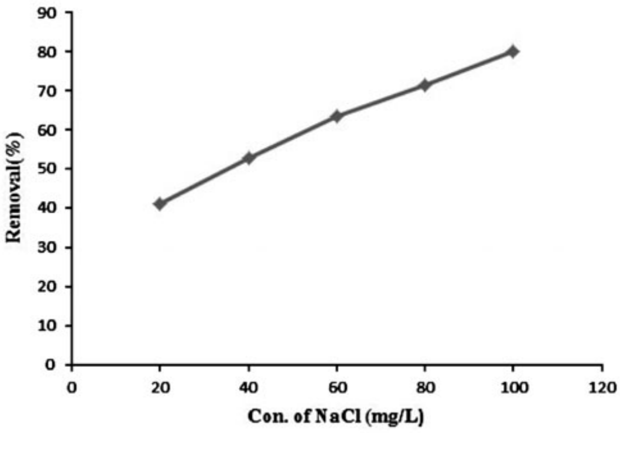

Fig. 6. Effect of ionic strength on the adsorption of lead ion onto PAN–TETA 100 (pH = 6, PAN–TETA = 0.1 g, agitation time = 1 h, $T = 20^\circ C$, $[\text{metal ions}]_0 = 25\,\text{mg L}^{-1}$).

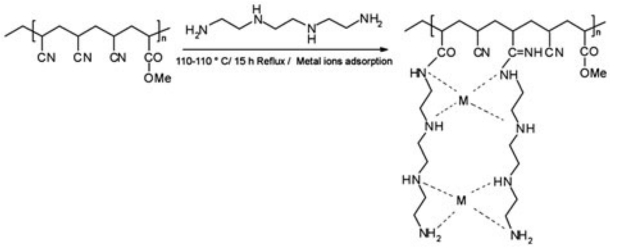

Fig. 7. Scheme of PAN–TETA 50 synthesized and the interaction with metal ions (M).

3.4. *Kinetics of adsorption*

The experimental data of silver and lead ions adsorption on the modified PAN in different time intervals were examined to fit pseudo-first-order, pseudo-second-order, and intraparticle diffusion kinetic models using the plots of $\ln(q_e - q_t)$ vs. t, t/q_t vs. t and q_t vs. $t^{1/2}$, respectively. The corresponding results are shown in Table 2(a) and (b). It is seen that the pseudo-second-order model well represented the

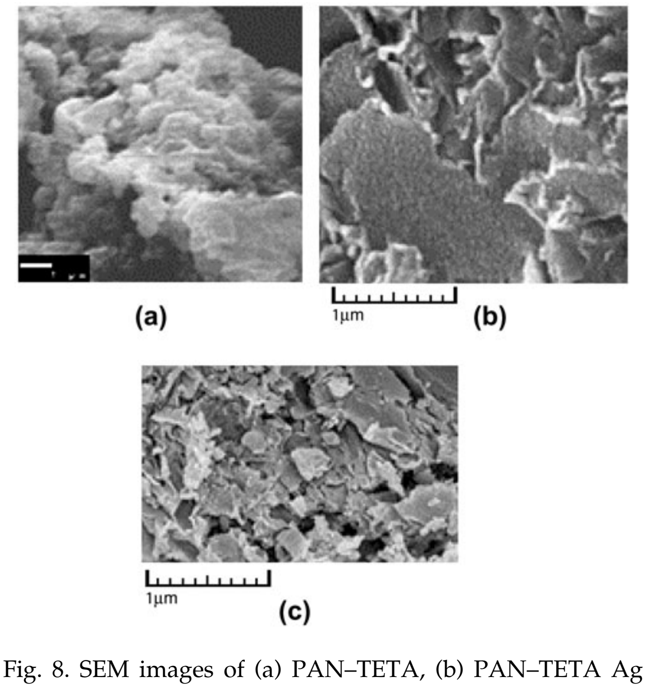

Fig. 8. SEM images of (a) PAN–TETA, (b) PAN–TETA Ag (I), and (c) PAN–TETA Pb(II).

Table 1
FTIR adsorption signals (cm^{-1}) for PAN–TETA and its metal complexes in maximum metal sorption

	NH_2–NH (stretching)	C–H (stretching)	C≡N (stretching)	C=O or C=N	N–H (bending)	C–H (bending)
PAN	–	2,939	2,245	1,628	–	1,072
PAN–TETA 50	3,394	2,931	2,245	1,651	1,556	1,057
PAN–TETA 100	3,371	2,932	–	1,651	1,559	1,057
PAN–TETA 50 Ag(I)	3,410	2,932	2,245	1,653	1,566	1,065
PAN–TETA 100 Ag(I)	3,418	2,932	–	1,651	1,597	1,065
PAN–TETA 50 Pb(II)	3,410	2,939	2,245	1,651	1,566	1,065
PAN–TETA 100 Pb(II)	3,418	2,932	–	1,651	1,505	1,065

Table 2
Adsorption kinetic parameters of silver ions (a) onto PAN–TETA 50 and 100 and lead ions (b) onto PAN–TETA 50 and 100

Sample	PAN–TETA 50 Ag(I)			PAN–TETA 100 Ag(I)			
Temperature (°C)	20	35	50	Temperature (°C)	20	35	50
Pseudo-first-order				*Pseudo-first-order*			
K_1, min^{-1}	0.023	0.015	0.010	K_1, min^{-1}	0.044	0.029	0.017
R^2	0.972	0.948	0.971	R^2	0.949	0.958	0.959
Pseudo-second-order				*Pseudo-second-order*			
K_2, $\text{g mg}^{-1}\ \text{min}^{-1}$	0.04	0.039	0.032	K_2, $\text{g mg}^{-1}\ \text{min}^{-1}$	0.043	0.039	0.044
$q_{e,\text{cal}}$ (mg g^{-1})	50.00	50.10	52.63	$q_{e,\text{cal}}$ (mg g^{-1})	50.00	50.12	52.63
$q_{e,\text{Exp}}$ (mg g^{-1})	49.28	50.21	51.14		49.71	50.38	51.29
R^2	1	1	1	R^2	1	1	1
Intraparticle diffusion				*Intraparticle diffusion*			
k_i, $\text{mg g}^{-1}\ \text{min}^{1/2}$	0.186	0.195	0.173	k_i, $\text{mg g}^{-1}\ \text{min}^{1/2}$	0.259	0.179	0.159
C	47.81	48.03	47.90	C	47.71	47.82	47.99
R^2	0.946	0.949	0.932	R^2	0.957	0.916	0.950
	PAN–TETA 50 Pb(II)			PAN–TETA 100 Pb(II)			
Pseudo-first-order				*Pseudo-first-order*			
K_1, min^{-1}	0.013	0.011	0.009	K_1, min^{-1}	0.004	0.003	0.001
R^2	0.940	0.940	0.951	R^2	0.985	0.978	0.982
Pseudo-second-order				*Pseudo-second-order*			
K_2, $\text{g mg}^{-1}\ \text{min}^{-1}$	0.005	0.004	0.003	K_2, $\text{g mg}^{-1}\ \text{min}^{-1}$	0.006	0.004	0.003
$q_{e,\text{cal}}$ (mg g^{-1})	47.61	50.00	50.00	$q_{e,\text{cal}}$ (mg g^{-1})	50.00	47.61	50.00
$q_{e,\text{Exp}}$ (mg g^{-1})	46.92	52.00	53.70		49.82	50.44	52.89
R^2	0.997	0.998	0.997	R^2	0.996	0.997	0.997
Intraparticle diffusion				*Intraparticle diffusion*			
k_i, $\text{mg g}^{-1}\ \text{min}^{1/2}$	0.947	1.073	1.019	k_i, $\text{mg g}^{-1}\ \text{min}^{1/2}$	0.945	1.001	1.020
C	35.22	36.11	35.64	C	34.79	35.11	36.00
R^2	0.961	0.985	0.974	R^2	0.968	0.943	0.959

experimental data ($R^2 > 0.99$). For instance, Fig. 9 shows the pseudo-second-order curves of PAN–TETA 100 with lead ions in the various temperatures. The theoretical q_e values for the silver and lead ions were also very close to the experimental q_e values in the case of pseudo-second-order equation (Table 2(a) and (b)). It is clear from the accuracy of the model that the adsorption kinetic of the silver and lead ions is described by a pseudo-second-order chemical reaction and that, this reaction is significant in the rate-controlling step. Physical adsorption and chemisorption may be indistinguishable in certain situations, and in some

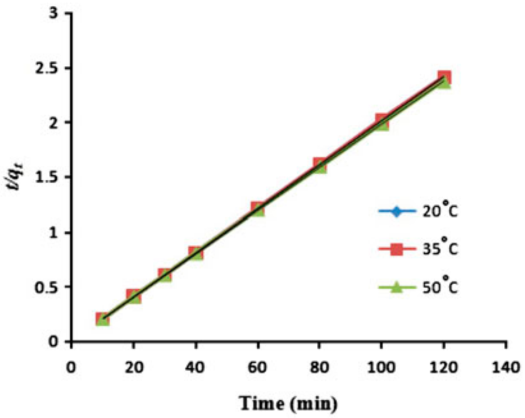

Fig. 9. Pseudo-second-order plots for the adsorption of lead ions onto PAN–TETA at various temperatures ([metal ions]$_0$ = 50 mg L^{-1}, PAN–TETA = 0.1 g, pH = 6).

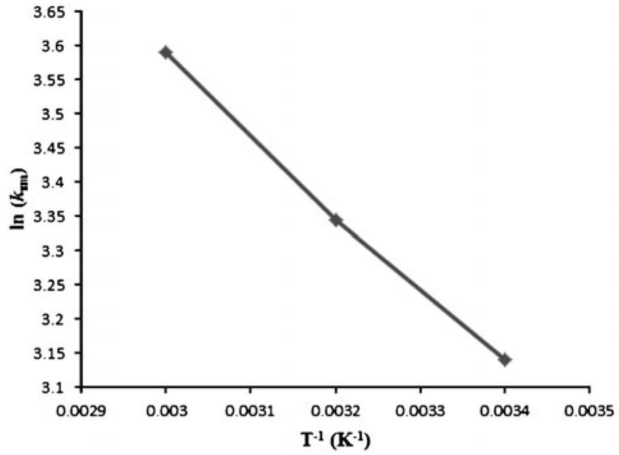

Fig. 10. plot of ln k_{sm} vs. T^{-1}: estimation of the activation energy, E_a, for the dsorption of silver ion onto PAN–TETA.

cases, a degree of both types of bondings can be presented at the same time, as with covalent bonds between two atoms having some degree of ionic character and vice versa [24].

3.5. Activation parameters

From three of the pseudo-second-order rate constants, k_2 (here K_{sm}), each obtained at a different temperature and using the Arrhenius equation (Eq. (5)), it is possible to gain some insight into the type of adsorption.

$$\ln k_{sm} = \ln A - E_a/RT \tag{6}$$

Here E_a is the activation energy (J mol^{-1}), k_{sm} the pseudo-second-order rate constant for adsorption (g mol^{-1} s^{-1}), A the temperature-independent Arrhenius factor (g mol^{-1} s^{-1}), R the gas constant (8.314 J K^{-1} mol^{-1}), and T the solution temperature (K). The slope of the plot of ln k_{sm} vs. T^{-1} can then be used to evaluate E_a (Fig. 10). Low activation energies (5–40 kJ mol^{-1}) are characteristic of physical adsorption, while higher ones (40–800 kJ mol^{-1}) suggest chemisorption [25]. The current results give $E_a = \sim +7.06$ kJ mol^{-1} for the adsorption of metal ions onto PAN–TETA indicating that the adsorption has a low potential barrier and corresponds to physisorption. The value is consistent with those found in the literature for the adsorption of these metal ions onto many adsorbents, e.g. Pb(II) onto poly(ethylene terephthalate)-g-acrylamide fibers [26], Pb(II) onto multi-amine-grafted mesoporous silicas [27], and lead ion into polymer-grafted banana (*Musa paradisiaca*) stalk [28].

3.6. Adsorption isotherms

The adsorption equilibrium isotherm is important for describing how the adsorbate molecules distribute between the liquid and the solid phases when the adsorption process reaches an equilibrium state. Thus, the correlation of equilibrium data using either a theoretical or empirical equation is essential for adsorption data interpretation and prediction. Several mathematical models can be used to describe experimental data of adsorption isotherms. Three frequently applied isotherm equations, the Langmuir, Freundlich, and Temkin were employed for further interpretation of the obtained adsorption data. One of the important steps for establishing a model that could be suitable for design purposes is the analysis of the isotherm data. It is done by checking how well they can be accommodated by different models. When the rate of molecules adsorption onto a surface is equal to the rate at which they are desorbed, adsorption equilibrium is achieved. At equilibrium, no change can be observed in the concentration of the solute on the solid surface or in the bulk solution, a situation characteristic of the entire system, including solute, adsorbent, solvent, temperature, pH, and so on [29].

The amount of metal ions adsorbed is determined as a function of the concentration at a constant temperature, which could be explained by adsorption isotherms. In this study, three isotherms Langmuir (Eq. (7)) [30], Freundlich (Eq. (8)) [31], and Temkin (Eq. (9)) [32] were tested.

$$\frac{C_e}{q_e} = \frac{1}{K_L} + \frac{a_L}{K_L} C_e \tag{7}$$

$$\log q_e = \log K_F + \frac{1}{n}\log C_e \tag{8}$$

$$q_e = B_1 \ln K_T + B_1 \ln C_e \tag{9}$$

Here q_e is the solid-phase equilibrium concentration, i.e. the amount of metal ions adsorbed per unit weight of the PAN–TETA (mg g^{-1}); C_e is the liquid-phase equilibrium concentration (mg L^{-1}), and K_L and a_L are Langmuir constants found from the intercept and slope of the straight line of the plot C_e/q_e vs. C_e. The a_L constant is related to the free energy or net enthalpy of adsorption (L mg^{-1}) ($a_L \propto e^{-\Delta H/RT}$) [33], and K_L is the equilibrium constant of Langmuir (L g^{-1}).

Freundlich constant indicative of the relative adsorption capacity of the adsorbent (mg g^{-1}) and $1/n$ is the adsorption intensity. $B_1 = RT/b$, K_T is the equilibrium binding constant (L mg^{-1}) and B_1 is the heat of adsorption (Eq. (8)).

Fig. 11 shows the Langmuir plot for the adsorption of lead ion onto PAN–TETA 100 at 20, 35, and 50°C as reproduced by the linearized Langmuir equation (Eq. (6)) and the best straight lines representing the fitted points. Hence, it is evident that the equilibrium data are accommodated well by the Langmuir model with high correlation coefficients as shown in Table 3. Such coefficients are indicative of monolayer coverage of the metal ions on the outer surface of the PAN–TETA molecules with maximum adsorption capacity (Table 3 (a) and (b)). These results demonstrate that the surface of PAN–TETA is homogeneous and a monolayer of metal ions covers the surface after adsorption.

Also, the essential characteristic of a Langmuir isotherm related to the isotherm shape can be expressed in terms of a dimensionless constant separation factor, also called the equilibrium parameter [31], R_L, which is defined in relation to a_L and C_0 as:

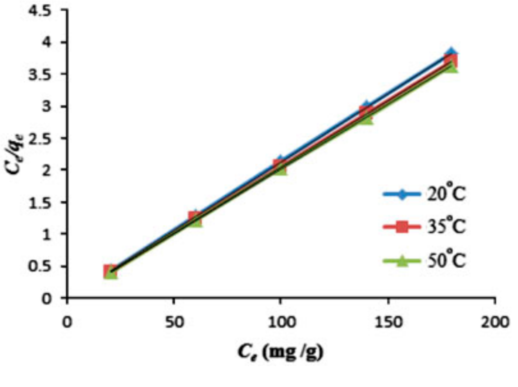

Fig. 11. Langmuir plot of adsorption of lead ions onto PAN–TETA at various temperatures (PH = 6, PAN–TETA = 0.1 g, $[\text{metal ions}]_0$ = 20, 60, 100, 140, and 180 mg L^{-1}).

$$R_L = \frac{1}{1 + a_L C_0} \tag{10}$$

The value of R_L indicates the type of the isotherm to be (i) unfavorable ($R_L > 1$), (ii) linear ($R_L = 1$), (iii) favorable ($0 < R_L < 1$), or (iv) irreversible ($R_L = 0$) [34]. The degree of favorability is generally related to the irreversibility of the system giving a qualitative assessment of the two metal ions and PAN–TETA (50 and 100) interactions.

The standard deviation is a measure of how precise the average is, that is, how well the individual numbers agree with each other. It is a measure of a type of error called random error—the kind of error that cannot be controlled very well. It is calculated as follows:

$$S = \sqrt{\frac{\sum (Xi - \bar{X})^2}{n - 1}} \tag{11}$$

Here, $\bar{X}$ is the average result and n is sum of the individual results. The calculated amount of standard deviation of relative errors for three models is shown in Table 3(a) and (b). Based on the data in Table 3, Langmuir is the best-fitting isotherms that had the highest coefficient of determination compared with the other methods.

Also, it is better to use the coefficient of determination of the linear and nonlinear regression method for comparing the best-fitting isotherms. Isotherm parameters obtained using the nonlinear method was calculated using SPSS 16 software (Table 4). It is obvious that there is the best correlation between linear and nonlinear data for the Langmuir isotherm [35].

3.7. Adsorption thermodynamics

The amount of metal ions adsorbed at equilibrium at different temperatures for 293.15, 313.15, and 333.15 K was examined to obtain thermodynamic parameters. Changes in the free energy (ΔG°), enthalpy (ΔH°), and entropy (ΔS°) were carried out with the following equations:

$$\Delta G^\circ = -RT \ln K_L \tag{12}$$

$$\Delta G^\circ = \Delta H^\circ - T\Delta S^\circ \tag{13}$$

where K_L is Langmuir constant when concentration terms are expressed in L mol^{-1}, R ($8.314\ \text{J mol}^{-1}\ \text{K}^{-1}$) is the universal gas constant, and T (K) is the temperature. The ΔH° and ΔS° values can be calculated from the slope and intercept of the plot of ΔG° vs. T (Eq. (12)).

Table 3
a) The adsorption parameters of Langmuir, Freundlich, and Temkin for PAN–TETA Ag(I) and b) for PAN–TETA Pb(II) at different temperatures

	Langmuir						Freundlich				Temkin			
Temperature (°C)	K_L	a_L	q_e (mg g^{-1})	R_L	R^2	Se	$1/n$	K_F	R^2	Se	B_1	K_T	R^2	Se
PAN–TETA 50 Ag(I)														
20	500	10	50.01	0.0019	1	0.00778	0.199	26.12	0.933	0.115	10.78	4.31	0.893	0.341
35	166.6	3.16	52.20	0.0062	0.999	0.01232	0.372	15.59	0.950	0.211	–	–	–	–
50	125	2.37	54.89	0.0083	0.999	0.01126	0.411	13.70	0.924	0.256	–	–	–	–
PAN–TETA 100 Ag(I)														
20	434	8.69	52.23	0.0029	1	0.00595	0.278	21.03	0.981	0.148	10.91	1.32	0.899	0.319
35	151.5	2.87	54.08	0.0069	1	0.03171	0.302	19.40	0.962	0.248	–	–	–	–
50	121.9	2.31	56.89	0.0085	0.999	0.07732	0.333	18.19	0.978	0.269	–	–	–	–
PAN–TETA 50 Pb(II)														
20	166	3.5	46.88	0.0058	0.999	0.00778	0.189	21.67	0.924	0.151	6.58	4.03	0.907	0.368
35	133.3	2.66	48.23	0.0074	0.999	0.01232	0.537	7.04	0.967	0.181	–	–	–	–
50	119	2.38	49.12	0.0083	1	0.01126	0.553	6.12	0.972	0.217	–	–	–	–
PAN–TETA 100 Pb(II)														
20	434.7	9.13	47.22	0.0021	1	0.00429	0.216	21.87	0.930	0.148	7.66	3.02	0.886	0.394
35	357.1	7.14	49.45	0.0027	0.997	0.00209	0.345	17.20	0.970	0.199	–	–	–	–
50	258.7	5.71	50.62	0.0034	0.999	0.00189	0.367	16.18	0.981	0.251	–	–	–	–

Table 4
Isotherm parameters obtained using the nonlinear method

	PAN–TETA 50 Ag(I)						PAN–TETA 100 Ag(I)					
	Langmuir			Freundlich			Langmuir			Freundlich		
Temperature (°C)	K_a	a_L	R^2	K_F	$1/n$	R^2	K_a	a_L	R^2	K_F	$1/n$	R^2
20	357.14	7.22	0.994	29.51	0.344	0.938	585.27	12.02	0.996	69.18	0.427	0.960
35	148.14	2.93	0.998	6.62	0.705	0.946	330.78	6.90	0.998	28.12	0.753	0.942
50	121.21	2.32	0.997	4.78	1.01	0.950	158.49	3.40	0.998	7.29	0.863	0.939
	PAN–TETA 50 Pb(II)						PAN–TETA 100 Pb(II)					
20	182.92	4.18	0.999	50.22	0.534	0.966	363.29	8.15	0.997	30.19	0.344	0.920
35	107.69	2.86	0.998	7.35	0.769	0.958	266.66	5.38	0.999	8.93	0.540	0.935
50	58.66	2.00	0.999	4.65	0.910	0.948	215.31	5.04	0.997	6.02	0.813	0.945

$$\ln K_L = -\Delta H^\circ/RT + \Delta S^\circ/R \qquad (14)$$

On the basis of a plot of ln K_L vs. T^{-1} (Eq. (11)), ΔH° can be estimated from the slope and ΔS° from the intercept of what should be a straight line passing through the points. The ΔH° and ΔS° values are thus found to be +16.28 – +18.49 and +75.36 – +78.31 J K^{-1}, respectively, while the ΔG° value is −4.16 to −6.75 kJ mol^{-1}. The free energy changes (ΔG°) are negative indicating the spontaneity and feasibility of these processes. The decrease in ΔG° value with increasing temperature reveals that adsorption of metal ions onto PAN–TETA becomes more favorable at higher temperature. The positive value of ΔH° further confirms that the adsorption processes are endothermic in nature [34]. The positive value of ΔS° infers increase of randomness at solid–solution interface during the adsorption of metal ions on the active sites of PAN–TETA. Moreover, positive value of ΔS° reflects the affinity of the adsorbent for metal ions [33].

3.8. Ion exchange capacity and swelling behavior of PAN–TEA

The maximum capacity of amine was obtained approximately as 5.9 mmol g^{-1} for PAN–TETA 50 and 8.64 mmol g^{-1} for PAN–TETA100. Moreover, swelling behavior of PAN–TETA 50 and PAN–TETA 100 were found 3 and 3.7%, respectively.

3.9. Desorption studies

Whether an adsorbent is an appropriate material in removal of metal ions from aqueous solutions depends not only on its adsorptive capacity, but also on its regeneration ability. For repeated use of an adsorbent, adsorbed metal ions should be easily desorbed under suitable conditions. Desorption studies help to elucidate the nature of adsorption and recycling of the spent adsorbent, silver, and lead ions. If the adsorbed metal ions can be desorbed using neutral pH water, then the attachment of the metal ions of the adsorbent is with weak bonds. If sulfuric acid or alkaline water desorbs the metal ions, then the adsorption is by ion exchange. If organic acids like acetic acid can desorb the metal ions, then the metal ions are held by the adsorbent through chemisorption [36,37]. The effect of various reagents used for desorption studies indicate that hydrochloric acid is a better reagent for desorption because we could get more than 91% removal of adsorbed heavy metal ions (Table 5). The reversibility of adsorbed silver and lead ions in mineral acid or base is in agreement with the pH-dependent results obtained. The desorption of

Table 5
Desorption percentage (%) of the metal ions using 1 M HCl as eluent

Reuse time	Recovery (%)
First	91.6
Second	93
Third	92.6

metal ions by mineral acids and alkaline medium indicates that the metal ions were adsorbed onto PAN–TETA through by physisorption mechanisms. As a result, the amount of activation energy and desorption studies confirm that adsorption has a low potential barrier and corresponds with physisorption.

3.10. Competitive Adsorption

In this group of experiments, competitive adsorption of Ag(I) and Pb(II) ions from their binary solutions was investigated. The initial concentration of each metal ion in the mixed solution was 25 mg L^{-1}. The solution was treated with 0.1 g of PAN–TETA for 30 min at pH 6.0 and at a temperature of 20°C.

As can be seen from Fig. 12, the amount of adsorbed Ag(I) ion was higher in terms of weight. The amounts of Ag(I) and Pb(II) ions adsorbed were 23.33 (removal 93.32%) and 14.29 mg (57.16% removal) per gram of PAN–TETA, respectively. Competitive adsorption of these metal ions from their binary solutions implied that only high-affinity sorption sites can adsorb silver ion when some adsorption sites are occupied by lead ion in solution [38]. Therefore, it is almost impossible to generalize the order of adsorption or define the extent of adsorption for each metal ion when they compete.

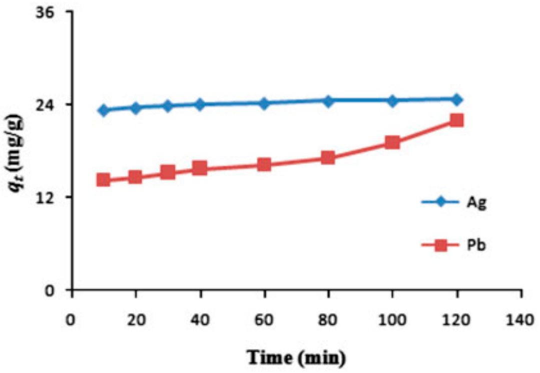

Fig. 12. Effect of contact time on the removal efficiency of silver and lead ions at room temperature ([metal ions]$_0$ = 50 mg L^{-1}, PAN–TETA = 0.1 g, pH = 6.0).

4. Conclusion

In the present study, the removal of metal ions from aqueous solutions was investigated by utilizing modified-PAN. PAN–TETA has been demonstrated to be highly effective for the removal of heavy metal ions from aqueous solutions. The adsorption equilibrium was attained within a time of less than 30 min. The best-fit adsorption isotherm was achieved with the Langmuir and not the Freundlich and Temkin models indicating that homogeneous adsorption occurs. The enthalpy change for the adsorption process (16.28–18.49 kJ mol^{-1}) confirms the endothermic nature of adsorption, while a free energy change in the range −4.16 to −6.75 kJ mol^{-1} confirms the spontaneity of the process. The competitive adsorption tests verified that these PAN–TETA had good adsorption selectivity for Ag (I) with the coexistence of Pb(II) and Ag(I). The order of affinity based on weight uptake by PAN–TETA (50 and 100) were Ag(I) > Pb(II). It is expected that the modified PAN can be used as an unconventional adsorbent for the removal of heavy metal ions from aqueous solutions.

References

[1] (a) L.H. Huang, Y.Y. Sun, Q.K. Yue, Q. Yue, L. Li, B. Gao, Adsorption of Cd(II) on lotus stalks-derived activated carbon: Batch and column studies, Desalin. Water Treat. 41(2012) 122–130; (b) Q. Yang, J. Zhang, Q. Yang, Y. Yu, G. Yang, Behavior and mechanism of Cd(II) adsorption on loess-modified clay liner, Desalin. Water Treat. 39(2012) 10–20.
[2] B.F. Senkal, N. Bicak, Glycidyl methacrylate based polymer resins with diethylene triamine tetra acetic acid functions for efficient removal of Ca(II) and Mg(II), React. Funct. Polym. 49 (2001) 151–157.
[3] G.R. Kiani, N. Arsalani, Synthesis and properties of some transition metal complexes with water soluble hydroxy functionalized polyacrylonitrile, Iran. Polym. J. 15 (2006) 727–735.
[4] G.R. Kiani, H. Sheikhloie, N. Arsalani, Heavy metal ion removal from aqueous solutions by functionalized polyacrylonitrile, Desalination 269 (2011) 266–270.
[5] N. Arsalani, M. Hosseinzadeh, Synthesis and characterization of EDTA functionalized polyacrylonitriles and their metal complexes, Iran. Polym. J. 14 (2004) 345–352.
[6] A. Barsanescu, R. Buhaceanu, V. Dulman, I. Bunia, V. Neagu, Adsorption of Zn(II) by crosslinked acrylic copolymers with amine functional groups, J. Appl. Polym. Sci. 93 (2004) 803–808.
[7] T.A. Kurniawan, G.Y.S. Chan, W.H. Lo, S. Babel, Physico-chemical treatment techniques for wastewater laden with heavy metals, Chem. Eng. J. 118 (2006) 83–98.
[8] Z. Yu, R. Wu, M. Wu, L. Zhao, R. Li, H. Zou, Preparation of polyamine-functionalized copper specific adsorbents for selective adsorption of copper, Colloids Surf. B 78 (2010) 222–228.
[9] C. Xiong, C. Yao, Synthesis, characterization and application of triethylenetetramine modified polystyrene resin in removal of mercury, cadmium and lead from aqueous solutions, Chem. Eng. J. 155 (2009) 844–850.
[10] L. Vinícius, A. Gurgel, L. Frédéric Gil, Adsorption of Cu(II), Cd(II), and Pb(II) from aqueous single metal solutions by succinylated mercerized cellulose modified with triethylenetetramine, Carbohydr. Polym. 77 (2009) 142–149.

[11] C. Liu, R. Bai, L. Hong, T. Liu, Functionalization of adsorbent with different aliphatic polyamines for heavy metal ion removal: Characteristics and performance, J. Colloid Interface Sci. 345 (2010) 454–460.

[12] X.Q. Sun, B. Peng, Y. Jing, J. Chen, D.Q. Li, Chitosan (chitin)/cellulose composite biosorbents prepared using ionic liquid for heavy metal ions adsorption, AlchE J. 55 (2009) 2062–2069.

[13] D. Zach-Maor, R. Semiat, H. Shemer, Removal of heavy metals by immobilized magnetite nano-particles, Desalin. Water Treat. 31 (2011) 64–70.

[14] N. Balkaya, T. Bektas, Chromium(VI) sorption from dilute aqueous solutions using wool, Desalin. Water Treat. 3 (2009) 43–52.

[15] M. Dogan, M. Alkan, Adsorption kinetics of methyl violet onto perlite, Chemosphere 50 (2003) 517–528.

[16] V.C. Taty-Costodes, H. Fauduet, C. Porte, A. Delacroixs, Removal of Cd(II) and Pb(II) ions from aqueous solutions by adsorption onto sawdust of *Pinus sylvestris*, J. Hazard. Mater. 105 (2003) 121–142.

[17] A.V. Borhade, A.G. Dholi, S.G. Wakchaure, Tope chemical modification of coal fly ash into iodate sodalite and its use for the removal of Cd^{2+}, Pb^{2+}, and Zn^{2+} from their aqueous solutions, Desalin. Water Treat. 50 (2012) 157–169.

[18] M. Dogan, M. Alkan, A. Turkyılmaz, Y. Ozdemir, Kinetics and mechanism of removal of methylene blue by adsorption onto perlite, J. Hazard. Mater. 109 (2004) 141–148.

[19] N. Arsalani, R. Rakh, E. Ghasemi, A.A. Entezami, Removal of Ni(II) from synthetic solutions using new amine-containing resins based on polyacrylonitrile, Iran. Polym. J. 16 (2009) 623–632.

[20] G.R. Mahdavinia, A. Pourjavadi, H. Hosseinzadeh, M.J. Zohuriaan, Modified chitosan 4. Superabsorbent hydrogels from poly(acrylic acid-co-acrylamide) grafted chitosan with salt- and pH-responsiveness properties, Eur. Polym. J. 40 (2004) 1399–1407.

[21] Y. Seki, K. Yurdakoc, Adsorption of promethazine hydrochloride with KSF montmorillonite, Adsorption 12 (2006) 89–100.

[22] A. Shukla, Y.H. Zhang, P. Dubey, J.L. Margrave, S.S. Shukla, The role of sawdust in the removal of unwanted materials from water, J. Hazard. Mater. 95 (2002) 137–152.

[23] I.B. Palheiros, A.C. Duarte, J.P. Oliveira, A. Hall, The influence of pH, ionic strength and chloride concentration on the adsorption of cadmium by a sediment, Water Sci. Technol. 21 (1989) 1873–1876.

[24] E. Bulut, M. Özacar, I. Ayhan Sengil, Adsorption of malachite green onto bentonite: Equilibrium and kinetic studies and process design, Micropor. Mesopor. Mater. 115 (2008) 234–246.

[25] X. Wang, A. Wang, Equilibrium isotherm and mechanism studies of Pb(II) and Cd(II) ions onto hydrogel composite based on vermiculite, Desalin. Water Treat. 48 (2012) 38–49.

[26] R. Coskun, C. Soykan, Lead(II) adsorption from aqueous solution by poly(ethylene terephthalate)-g-acrylamide fibers, J. Polym. Res. 13 (2006) 1–8.

[27] L. Zhang, C. Yu, W. Zhao, Z. Hua, H. Chen, L. Li, J. Shi, Preparation of multi-amine-grafted mesoporous silicas and their application to heavy metal ions adsorption, J. Non-Cryst. Solids 353 (2007) 4055–4061.

[28] I.G. Shibi, T.S. Anirudhan, Polymer-grafted banana (*Musa paradisiaca*) stalk as an adsorbent for the removal of lead(II) and cadmium(II) ions from aqueous solutions: Kinetic and equilibrium studies, J. Chem. Technol. Biotechnol. 81 (2006) 433–444.

[29] E.N.E. Qada, S.J. Allen, G.M. Walker, Adsorption of methylene blue onto activated carbon produced from steam activated bituminous coal: A study of equilibrium adsorption isotherm, Chem. Eng. J. 124 (2006) 103–110.

[30] I. Langmuir, The constitution and fundamental properties of solids and liquids. Part I. Solids, J. Am. Chem. Soc. 38 (1916) 2221–2295.

[31] H. Radnia, A. Asghar Ghoreyshi, H. Younesi, G.D. Najafpour, Adsorption of Fe (II) Ions from aqueous phase by chitosan adsorbent: Equilibrium, kinetic and thermodynamic studies, Desalin. Water Treat. 50 (2012) 348–359.

[32] G. Rytwo, R. Huterer-Harari, S. Dultz, Y. Gonen, Adsorption of fast green and erythrosin-B to montmorillonite modified with crystal violet, J. Therm. Anal. Calorim. 84 (2006) 225–231.

[33] R.A. Shawabkeh, M.F. Tutunji, Experimental study and modeling of basic dye sorption by diatomaceous clay, Appl. Clay Sci. 24 (2003) 111–120.

[34] Y. Ho, Isotherms for the sorption of lead onto peat: Comparison of linear and non-linear methods, Pol. J. Environ. Stud. 15 (2006) 81–86.

[35] Z.L. Zhao, X.Q. Wang, C. Zhao, X.G. Zhu, S.Y. Du, Adsorption and desorption of antimony acetate on sodium montmorillonite, J. Colloid Interface Sci. 345 (2010) 154–159.

[36] R. Laus, T.G. Costa, B. Szpoganicz, V.T. Favere, Adsorption and desorption of Cu(II), Cd(II) and Pb(II) ions using chitosan crosslinked with epichlorohydrintriphosphate as the adsorbent, J. Hazard. Mater. 183 (2010) 233–241.

[37] S.B. Chen, Y.B. Ma, L. Chen, K. Xian, Adsorption of aqueous Cd^{2+}, Pb^{2+}, Cu^{2+} ions by nano-hydroxyapatite: Single- and multi-metal competitive adsorption study, Geochem. J. 44 (2010) 233–239.